

# A current sensor fault diagnosis method based on phase angle shift technique applying to induction motor drive

Quang Sy Vu<sup>1</sup>, Cuong Dinh Tran<sup>2</sup>, Bach Hoang Dinh<sup>2</sup>, Chau Si Thien Dong<sup>3</sup>, Hung Tan Huynh<sup>3</sup>,  
Huy Xuan Phan<sup>4</sup>

<sup>1</sup>Faculty of Automotive Engineering, School of Engineering and Technology, Van Lang University, Ho Chi Minh City, Vietnam

<sup>2</sup>Power System Optimization Research Group, Faculty of Electrical and Electronics Engineering, Ton Duc Thang University, Ho Chi Minh City, Vietnam

<sup>3</sup>Faculty of Electrical and Electronics Engineering, Ton Duc Thang University, Ho Chi Minh City, Vietnam

<sup>4</sup>Long An Power Company, Tan An City, Vietnam

## Article Info

### Article history:

Received Apr 18, 2022

Revised May 25, 2022

Accepted June 29, 2022

### Keywords:

Current sensor fault  
Diagnosis algorithm  
Fault-tolerant control  
Phase angle shift  
Three-phase current

## ABSTRACT

An improved method using the phase angle shift characteristic of the sine wave is proposed to diagnose the fault states of the current sensors in an induction motor drive. The induction motor drive (IMD) system applied in this study uses the field-oriented control (FOC) loop with integrated two current sensors and a speed encoder to control the rotor speed. The space vectors created from the phase angle shift technique are compared to the estimated current for the fault diagnosis algorithm. Various types of current sensor failures are investigated by MATLAB/Simulink software to check the effectiveness of the proposed method. The simulation results have proved the performance of the proposed method in enhancing the reliability and stability of the IMD system.

*This is an open access article under the [CC BY-SA](https://creativecommons.org/licenses/by-sa/4.0/) license.*



## Corresponding Author:

Cuong Dinh Tran

Power System Optimization Research Group, Faculty of Electrical and Electronics Engineering

Ton Duc Thang University

19 Nguyen Huu Tho, District 7, Ho Chi Minh City, Vietnam

Email: trandinhcuong@tdtu.edu.vn

## NOMENCLATURE

$i_S^S / i_R^S$	Stator/ Rotor current vector in $[\alpha\beta]$
$\psi_S^S / \psi_R^S$	Stator/ Rotor flux vector in $[\alpha\beta]$
$u_{S\alpha}, u_{S\beta}$	Stator voltage components in $[\alpha\beta]$
$u_{Sx}, u_{Sy}$	Stator voltage components in $[xy]$
$i_{Sx} / i_{Sy}$	Flux current/ Torque current
$\omega_m$	Mechanical angular speed
$\omega_r$	Electrical angular speed
$\psi_{Rx}, \psi_{Ry}$	Rotor flux components in $[xy]$

## 1. INTRODUCTION

The three-phase induction motor with ideal size, low cost, and high durability is one of the most popular motor types in industrial applications. Robust developments in power electronics and soft computing have accelerated the penetration of the induction motor into speed control applications [1]. A modern

induction motor drive IMD system has four main parts: a power supply inverter, an induction machine, a soft computing controller, and feedback sensors. Control requirements such as flux and the motor speed will be set in the controller as reference signals. Besides, the sensors provide signs showing the instantaneous operating state of the IMD system to feedback to the controller. Control algorithms will use reference signals, feedback signals, and motor parameters to generate control commands for the switching process of the inverter, thereby providing the proper power to the motor.

Many effective methods have been researched and applied for speed control of IMD systems, divided into two significant families, including scalar control and vector control. Scalar control with the simple algorithm, the typical hardware configuration is appropriate for applications that do not need high precision [2]-[4]. In contrast, vector control is suitable for the speed control and torque control of high-performance applications [5]. One of the typical vector control techniques is the field-oriented control (FOC) method, which can precisely control flux and moment based on the stator current separation technique [6]. Based on the control method of the separately excited direct current DC motor, the stator current vector is separated into two perpendicular components in the rotation coordinate system  $[xy]$ , whose x-axis is the axis corresponding to the rotor flux [7]-[9]. The current component on the x-axis is used to maintain the rotor flux as a constant during operation. Otherwise, the current on the y-axis is applied to adjust the electrical torque for the speed control of IMD [10], [11].

The feedback current and rotor speed from sensors play a core role in the success of the FOC control method. Inaccuracy of the feedback signals can cause instability in the operation of the drive system, and in severe cases, it can damage equipment and lead to negative economic impacts. In recent years, sensor fault-tolerant control (FTC) methods have been focused on improving the reliability and stability of IMD systems [12]. FTC techniques are usually divided into two groups, Passive FTC and Active FTC [13]. Conventional passive FTC techniques are incorporated in the general function of the controller to handle a predefined number of sensor failures. Active FTC techniques focus on diagnosing the fault types, determining the faulty sensor, performing false signal isolation, and reconfiguring the control system. Most speed sensor fault diagnosis uses the comparison methods of rotor speed signals such as reference speed, measured speed, and estimated speed to determine the speed sensor fault [14]. Meanwhile, the current sensor's fault diagnosis and identification techniques have been studied in various ways and different approaches. Therefore, this study focuses on researching solutions for diagnosing current sensor faults in IMD systems controlled by the FOC method.

Current sensor failures occur in a variety and complexity, often divided into soft and hard fault types [13], [15]. Soft sensor faults can degrade the performance of the IMD system; if these faults occur for a long time, they can lead to severe impacts on the operation. Soft sensor fault type includes drift, bias, scaling faults, etc. Hard sensor fault, known as a complete failure, is a type of sensor fault where the signal is completely lost; this fault is very severe and can immediately negatively impact the system's operation. Hard sensor fault needs to be diagnosed and handled as soon as possible to ensure the safety of IMD.

Kirchoff's current law is often applied to detect and locate the faulty sensor [16]. However, the principle of Kirchoff's law is not possible to diagnose the faulty current sensor in an IMD using two current sensors. Najafabadi *et al.* [17], the authors use the difference between root mean square values of the phase currents and the estimated current to create the current indexes for current fault detection. This method diagnoses the current sensor accurately, but the fault diagnosis time is extended, especially in the low-speed zone. Chakraborty and Verma [18], the authors proposed an Axes transformation to detect the current sensor fault. The measured currents are transferred into two coordinate systems  $[\alpha\beta]$ , each with an  $\alpha$ -axis corresponding to each phase current. Besides, two estimators are also used to create the estimated currents from current components in the rotating frame  $[xy]$  of the FOC loop. In the respective coordinate systems, each pair of current vectors will be compared to determine the state of each current sensor. Yu *et al.* [19], the voltage in the system  $[abc]$  is transformed into the coordinate systems  $[\alpha\beta]$  corresponding to the phase currents. Therefore, the estimated current vectors will have an  $\alpha$ -axis corresponding to each measured current. The signals of the measured current, the estimated current, and the estimated flux are combined into a function for determining the state of each current sensor. Extended kalman filter (EKF) is applied to provide the estimated stator current for the diagnosis algorithms in the article [20]. In the healthy condition, the difference between sensor outputs and outputs of EKF is equal to zero. When the current sensor faults occur, leading to a higher residual than a predefined threshold, thus the wrong phase current can be detected. Tran *et al.* [21] proposed a current sensor fault diagnosis based on a sine waveform and space vector combination. The comparison between the sine current and its delay signal is applied to detect the hard sensor fault; besides, the comparison algorithm between the current space vectors is used to diagnose the soft sensor fault. The advantage of this method is to quickly detect sensor faults to ensure continuous and stable operation of the system.

This paper proposes a new approach for the current sensor fault diagnosis technique in an IMD system using two current sensors. Each phase current combines two  $\pm 120$  degree phase shift signals to create an independent measured current space vector. Besides, the mathematical model of the induction motor is also applied to estimate a virtual current space vector. The current space vectors will be compared to diagnose the fault condition and locate the faulty sensor accurately. After identifying the defective sensor, the FTC function isolates the failure signal from the control system. Virtual current signals that replace false signals are used in control algorithms to ensure the continuous and stable operation of the IMD [22]-[24]. The performance of the proposed method will be tested with various sensor fault types by MATLAB/Simulink software. The simulation results have proved the proposed method to accurately diagnose the fault status of the current sensors for both soft fault and hard fault.

## 2. DIAGNOSIS METHOD FOR CURRENT SENSOR FAULTS

The content in this section consists of two main parts: the mathematical model of the IMD system will be described in part one, and the diagnosis algorithm in part two.

### 2.1. Mathematical model of induction motor

The electromagnetic relationship in the induction motors is a complex nonlinear relationship described by differential equations in stationary coordinates  $[\alpha\beta]$  as:

$$u_s^S = R_S i_s^S + \frac{d\psi_s^S}{dt} \tag{1}$$

$$0 = R_R i_R^S + \frac{d\psi_R^S}{dt} - j\omega_r \psi_R^S \tag{2}$$

$$\psi_s^S = L_S i_s^S + L_m i_R^S \tag{3}$$

$$\psi_R^S = L_m i_s^S + L_R i_R^S \tag{4}$$

In this paper, the FOC technique is applied to precisely control the speed and torque for the IMD. The general block diagram of the IMD system using the FOC method for speed control is shown in Figure 1.

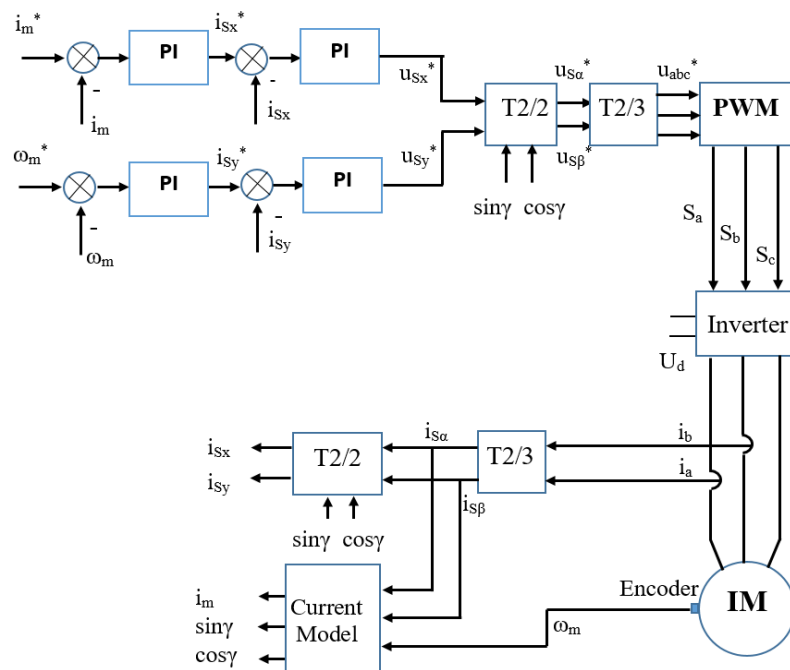


Figure 1. Block diagram of IMD using FOC

The three-phase current from the sensors will be transformed to a current space vector in a stationary coordinate system  $[\alpha\beta]$  and a rotating coordinate system  $[xy]$ . Clark's and Park's formulas [25] are used to analyze the current components in reference frame systems, corresponding to block T2/2 and T2/3.

$$\text{Clark's fomulas: } \begin{bmatrix} i_{S\alpha} \\ i_{S\beta} \end{bmatrix} = \begin{bmatrix} 1 & 0 \\ \frac{1}{\sqrt{3}} & \frac{2}{\sqrt{3}} \end{bmatrix} \begin{bmatrix} i_a \\ i_b \end{bmatrix} \quad (5)$$

$$\text{Park's fomulas: } \begin{bmatrix} i_{Sx} \\ i_{Sy} \end{bmatrix} = \begin{bmatrix} \cos \gamma & \sin \gamma \\ -\sin \gamma & \cos \gamma \end{bmatrix} \begin{bmatrix} i_{S\alpha} \\ i_{S\beta} \end{bmatrix} \quad (6)$$

Magnetic current “ $i_m$ ,” synchronous speed “ $\omega_e$ ,” rotor flux angle “ $\gamma$ ” are calculated through the IM current model. The stator current components in stationary coordinate  $[\alpha\beta]$  are converted into rotating coordinate  $[dq]$  corresponding to the rotor axis, as (7).

$$\begin{bmatrix} i_{Sd} \\ i_{Sq} \end{bmatrix} = \begin{bmatrix} \cos \varepsilon & \sin \varepsilon \\ -\sin \varepsilon & \cos \varepsilon \end{bmatrix} \begin{bmatrix} i_{S\alpha} \\ i_{S\beta} \end{bmatrix}$$

Where:

$$\varepsilon = \int \omega_r dt; \omega_r = p\omega_m \quad (7)$$

The components of “ $i_m$ ” in the rotor rotating coordinate  $[dq]$  system are calculated as in (8).

$$\begin{bmatrix} i_{md} \\ i_{mq} \end{bmatrix} = \begin{bmatrix} \frac{1}{T_{RS}+1} & 0 \\ 0 & \frac{1}{T_{RS}+1} \end{bmatrix} \begin{bmatrix} i_{Sd} \\ i_{Sq} \end{bmatrix} \quad (8)$$

The “ $i_m$ ” current in rotor rotating coordinate  $[dq]$  is transformed back to  $[\alpha\beta]$  system for determining the synchronous speed and rotor flux angle, as in:

$$\begin{bmatrix} i_{m\alpha} \\ i_{m\beta} \end{bmatrix} = \begin{bmatrix} \cos \varepsilon - \sin \varepsilon \\ \sin \varepsilon \cos \varepsilon \end{bmatrix} \begin{bmatrix} i_{md} \\ i_{mq} \end{bmatrix} \quad (9)$$

$$\begin{cases} \gamma = \arctg\left(\frac{i_{m\beta}}{i_{m\alpha}}\right) \\ i_m = \sqrt{(i_{m\alpha}^2 + i_{m\beta}^2)} \end{cases} \quad (10)$$

The PI controllers are applied in the FOC loop to modulate the deviations to become reference voltage signals. The PWM technique will modulate the reference voltage signal to create a switching pulse that drives the inverter for supplying power to the motor.

## 2.2. Current sensor fault diagnosis algorithm based on phase angle shift technique

Because the control principle is based on current space vector separation, the measured stator current plays a crucial role in IMD speed control using FOC method. Inaccuracy of the feedback current signals will seriously affect the control efficiency. An FTC function can be integrated into IMD's control system to enhance the reliability and stability of the system. A block diagram of the FOC integrated FTC function is shown in Figure 2.

The FTC unit receives the measured current and feedback speed signals to determine the state of the current sensors by the diagnosis algorithms. If the current sensors are healthy, the output current signal transfers to the FOC loop as the measured current signal. Otherwise, if the current sensors are damaged, the FTC will indicate the faulty sensor, and the output current will be the estimated current. Figure 3 presents a block diagram of the FTC unit. In steady-state, the rotor slip can be calculated from measured stator current, rotor speed, and time constant, as (11).

$$\omega_{sl} = \frac{i_{Sy}}{T_{R}i_{Sx}} \quad (11)$$

The electrical synchronous speed can be determined from the rotor speed and rotor slip, as in (12).

$$\omega_e = \omega_r + \omega_{sl} \quad (12)$$

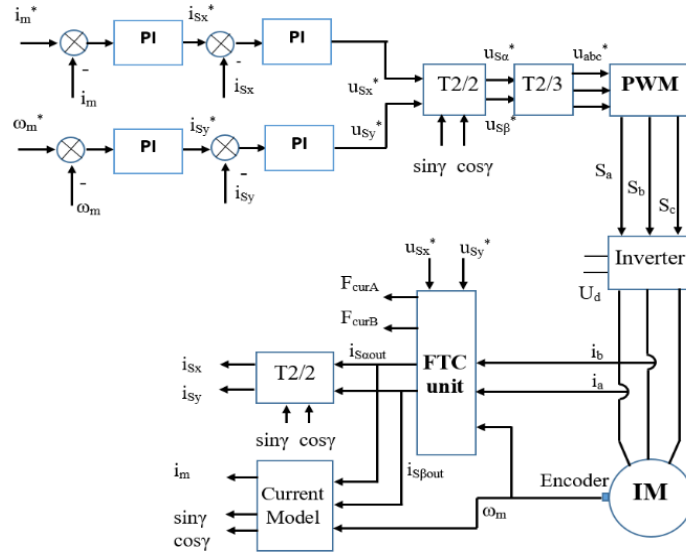


Figure 2. IMD applying FOC integrated FTC function

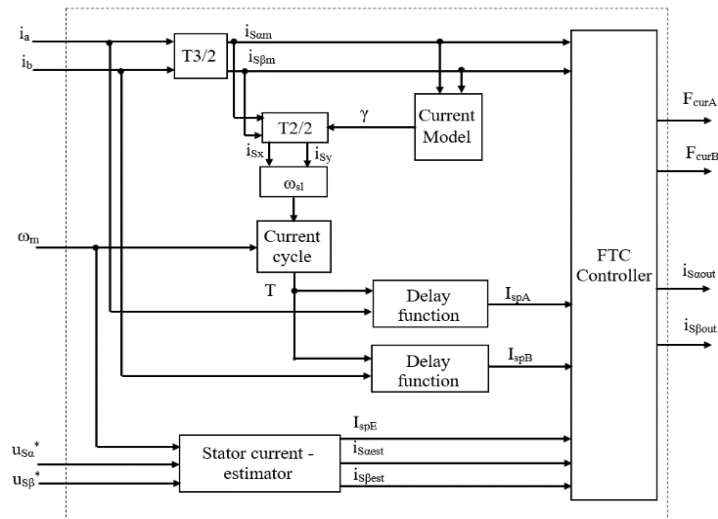


Figure 3. Block diagram of the FTC controller

In (13) presents the method of determining the current cycle corresponding to the actual operating speed of the IMD.

$$T = \frac{2\pi}{\omega_e} \tag{13}$$

Each phase current will be delayed, corresponding to  $T/3$  and  $2T/3$  to create two delay-currents, as shown in (14).

$$\begin{cases} i_j(n) = i_j(t) = I_m \sin(\omega_e t) \\ \text{Delay}[T/3]: i_j(n-1) = i_j(t - \frac{T}{3}) = I_m \sin(\omega_e(t - \frac{T}{3})) = I_m \sin(\omega_e t - \frac{2\pi}{3}) \\ \text{Delay}[2T/3]: i_j(n-2) = i_j(t - \frac{2T}{3}) = I_m \sin(\omega_e(t - \frac{2T}{3})) = I_m \sin(\omega_e t - \frac{4\pi}{3}) \end{cases} \tag{14}$$

These currents will be combined to generate a current space vector by formulas (15), (16).

$$\begin{bmatrix} i_{js\alpha} \\ i_{js\beta} \end{bmatrix} = \begin{bmatrix} \frac{2}{3} & -\frac{1}{3} & -\frac{1}{3} \\ 0 & \frac{1}{\sqrt{3}} & -\frac{1}{\sqrt{3}} \end{bmatrix} \begin{bmatrix} i_j(n) \\ i_j(n-1) \\ i_j(n-2) \end{bmatrix} \tag{15}$$

$$I_{spj} = \sqrt{i_{js\alpha}^2 + i_{js\beta}^2} \quad (16)$$

The proposed sensor fault diagnosis method is based on an algorithm comparing the magnitudes of the phase shift current vectors and the estimated current vector. During operation, the motor parameter variations by the influence of temperature will lead to the inaccuracy of the virtual current in the direct estimation methods. Therefore, the current estimation algorithm must be selected appropriately to avoid the excessive influence of the motor parameters. The Luenberger observer [23] using motor parameters and feedback rotor speed to estimate the virtual current vector could be considered a reasonable selection.

$$\begin{cases} \frac{di_{Saest}}{dt} = -Ai_{Saest} + B\psi_{Raest} + C\omega_r\psi_{R\beta est} + Du_{S\alpha} - H_1i_{Saest} + H_2i_{S\beta est} \\ \frac{di_{S\beta est}}{dt} = -Ai_{S\beta est} + B\psi_{R\beta est} - C\omega_r\psi_{Raest} + Du_{S\beta} - H_2i_{Saest} - H_1i_{S\beta est} \\ \frac{d\psi_{Raest}}{dt} = Ei_{Saest} - F\psi_{Raest} - \omega_r\psi_{R\beta est} - H_3i_{Saest} + H_4i_{S\beta est} \\ \frac{d\psi_{R\beta est}}{dt} = Ei_{S\beta est} - F\psi_{R\beta est} - \omega_r\psi_{Raest} - H_4i_{Saest} - H_3i_{S\beta est} \end{cases} \quad (17)$$

$$I_{spE} = \sqrt{i_{Saest}^2 + i_{S\beta est}^2}$$

Where:

$$\begin{aligned} A &= \frac{R_S L_R^2 + R_R L_m^2}{\sigma L_S L_R^2}; B = \frac{L_m R_R}{\sigma L_S L_R^2}; C = \frac{L_m}{\sigma L_S R_R}; \\ D &= \frac{1}{\sigma L_S}; E = \frac{L_m R_R}{L_R}; F = \frac{R_R}{L_R}; \sigma = \frac{L_S L_R - L_m^2}{L_S L_R}; \\ H_1 &= (g - 1) \left( \frac{1}{\sigma T_S} + \frac{1}{\sigma T_R} \right); H_2 = -(g - 1)\omega_r; H_4 = -(g - 1) \frac{\sigma L_S L_m}{L_R} \omega_r; \\ H_3 &= (g^2 - 1) \left[ \left( \frac{1}{\sigma T_S} + \frac{1}{\sigma T_R} \right) \frac{\sigma L_S L_m}{L_R} - \frac{L_m}{T_R} \right] + \frac{\sigma L_S L_m}{L_R} \left( \frac{1}{\sigma T_S} + \frac{1}{\sigma T_R} \right) (g - 1); \\ g &> 1; \end{aligned}$$

The magnitude of the current space vectors based on the phase angle shift technique will be compared with the magnitude of the virtual space vectors to determine the current sensor fault of each phase.

$$\begin{cases} \text{If } (|I_{spj} - I_{spE}| > \text{Threshold}) \\ \{F_{curj} = 1;\} \\ \text{Else} \\ \{F_{curj} = 0;\} \end{cases} \quad (18)$$

The ‘‘Threshold’’ value is the maximum difference between the phase shift current space vector and the estimated current vector in the healthy sensor condition. This value is an essential factor in determining the success of the diagnosis algorithm. Especially when a load change occurs suddenly, if the selected ‘‘Threshold’’ value is not suitable, the diagnosis method can confuse the transient operating condition with the sensor fault state, thus leading to make inappropriate control decisions. Based on many simulations performed, this study recommends a value of 15% of the rated current value for the Threshold. After diagnosing the failure current signal, the FTC unit will isolate and replace the fault signal with the estimated current and indicate the faulty current sensor to be fixed and replaced at an appropriate time.

### 3. SIMULATION RESULTS

An IMD model corresponding to the embedded FTC function of the FOC method in Figure 2 is applied to simulate the current sensor fault cases in the Matlab/Simulink environment. The parameter of the three-phase motor used in the simulations is present in Table 1, and the reference motor speed is depicted in Figure 4. Four types of current sensor failures will be diagnosed in this study, including total, scaling, bias, and drift failures.

First, the diagnosis algorithm will be implemented to determine the effectiveness against the total fault, a typical type of the hard sensor fault group. IMD applies the FOC method to control the rotor speed according to the reference speed. Assuming that the current of the A-phase sensor is completely damaged at 2 seconds, the value of the feedback current is equivalent to zero, as shown in Figure 5(a). The fault indication

flag of the A-phase is immediately set to a high level, while the flag of the B-phase remains at a low level, Figure 5(b). The fault diagnosis function immediately isolates the fault signal and replaces it with an estimated current to feed the FOC loop, as shown in Figure 5(c). Figure 5(d) has proved that the IMD system still maintains stable operation even in the current sensor fault condition.

Table 1. Parameters of three-phase motor

Description	Symbol	Unit	Value
Rated Torque	$T_r$	Nm	14.8
Rated Speed	$\omega_r$	rpm	1420
Rated current	$I$	A	4.85
Number of pole pairs	$p$	-	2
Stator/Rotor Resistance	$R_s/R_r$	$\Omega$	3.179/2.118
Magnetizing Inductance	$L_m$	H	0.192
Stator/Rotor Inductance	$L_s/L_r$	H	0.209/0.209

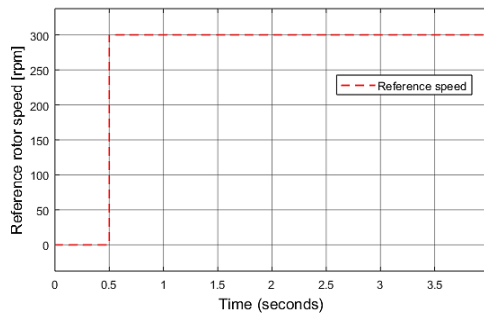


Figure 4. Reference speed for the simulations

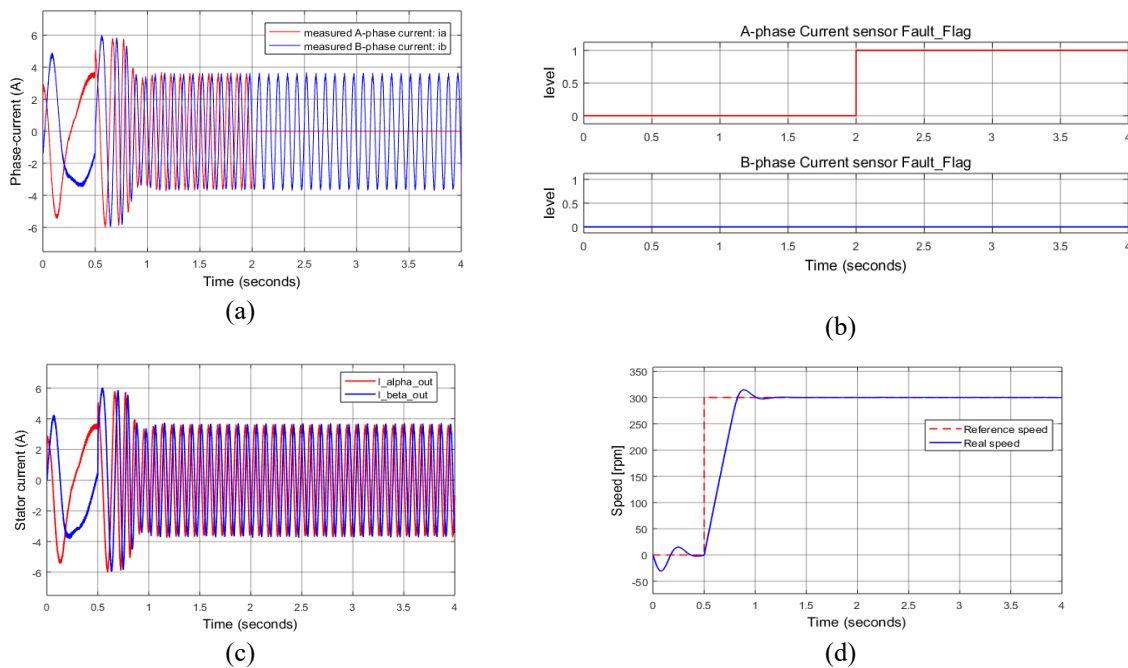


Figure 5. FTC against total fault: (a) measured current, (b) current sensor fault indication, (c) output current of FTC unit, and (d) rotor speed

Next, some soft sensor faults are investigated to verify the effectiveness of the proposed diagnosis method. At the 2-second time, scaling fault occurs at the B-phase sensor, and the amplitude of the B-phase current is amplified three times, as in Figure 6(a). As in the above case, the defective sensor is determined rapidly and accurately. Figures 6(b)-6(d) show that the IMD system operates stably and reliably. In the three-study, the diagnosis method is carried out for bias failure of the A-phase current sensor, and a value of

2 Amps biases the A-phase current at 2 seconds, as in Figure 7(a). The fault diagnosis function worked correctly, and the wrong signal was replaced by the estimated current corresponding to Figures 7(b), 7(c). The performance of the IMD system is firmly maintained against current sensor failure, as in Figure 7(d).

The drift fault is examined in case four. At 2s, B-phase current drifts, as shown in Figure 8(a). In the initial stage of the drift failure, the change of the B-phase current is still small. It has not seriously affected the operation of the system, so the system still maintains the process with the measured signal. However, when the deviation of the wrong signal increased to a level that could affect the stability of the IMD system, the diagnosis function detected and accurately located the fault, as shown in Figure 8(b). The FTC unit has provided proper output currents to the FOC loop to ensure the reliable stability of the system, as in Figures 8(c) and 8(d). The proposed algorithm has successfully diagnosed various types of sensor fault, including hard sensor fault and soft sensor fault. The proposed diagnosis method has proven its effectiveness in enhancing the reliability of the IMD system against current sensor faults.

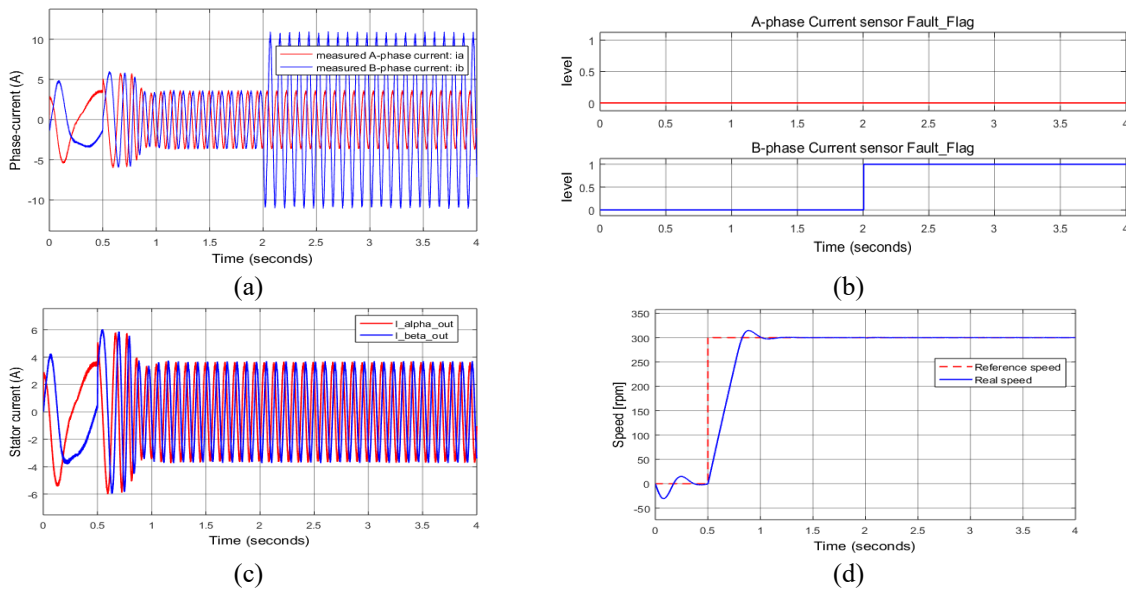


Figure 6. FTC against scaling fault: (a) measured current, (b) current sensor fault indication, (c) output current of FTC unit, and (d) rotor speed

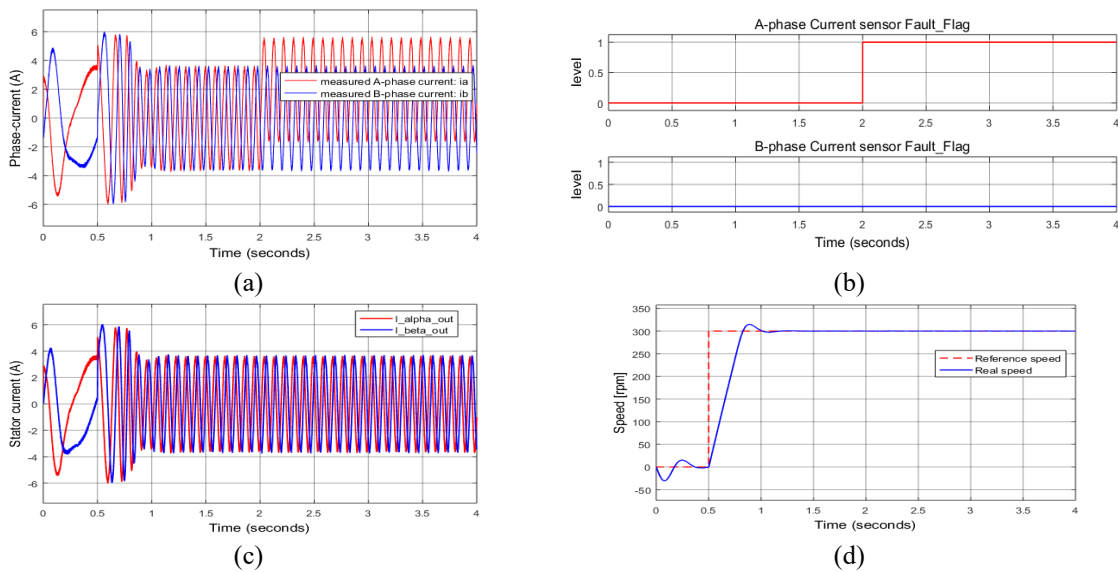


Figure 7. FTC against bias fault: (a) measured current, (b) current sensor fault indication, (c) output current of FTC unit, and (d) rotor speed

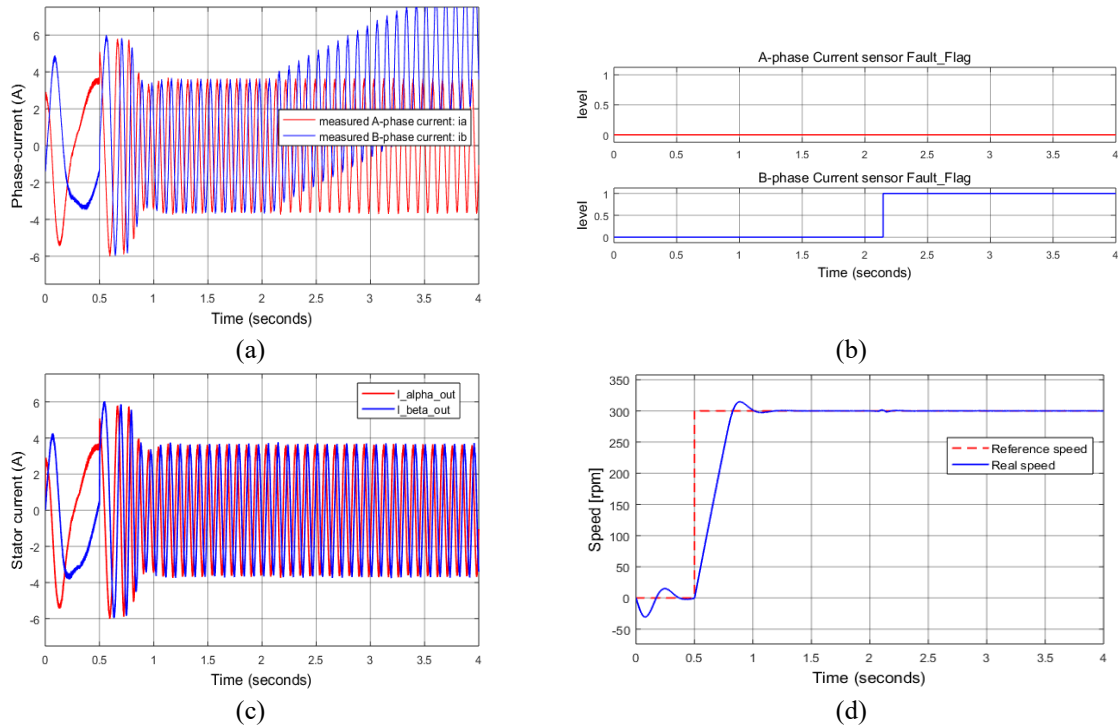


Figure 8. FTC against drift fault: (a) measured current, (b) current sensor fault indication, (c) output current of FTC unit, and (d) rotor speed

#### 4. CONCLUSION

A fault diagnosis method based on the phase shift technique is proposed to detect the current sensor faults during the operation of the IMD. Each measured current will be shifted its phase angle corresponding to  $T/3$  and  $2T/3$  to create two delay-currents. As a result, the measured space vector is formed from each phase current and its two delay phases. The magnitude of each measured current vector will be compared with the estimated current to determine the operation state of the current sensors. The simulation results proved that the proposed algorithm effectively detects current sensor fault types, including hard and soft faults. The IMD system still maintains stable operation when the current sensor fault occurs; the indication flags accurately identify the fault phase. Corresponding faulty current sensors will be fixed or replaced at the appropriate time.

#### ACKNOWLEDGEMENTS

The authors would like to thank Ton Duc Thang University and Van Lang University, Vietnam.

#### REFERENCES

- [1] R. E. Araújo, "Induction motors: Modelling and control." *InTech*, Croatia, 2012.
- [2] J. M. Peña and E. V. Díaz, "Implementation of V/f scalar control for speed regulation of a three-phase induction motor," *IEEE ANDESCON*, 2016, pp. 1-4, doi: 10.1109/ANDESCON.2016.7836196.
- [3] Z. Zhang and A. M. Bazzi, "Robust Sensorless Scalar Control of Induction Motor Drives with Torque Capability Enhancement at Low Speeds," *IEEE International Electric Machines & Drives Conference (IEMDC)*, 2019, pp. 1706-1710, doi: 10.1109/IEMDC.2019.8785159.
- [4] T. H. D Santos, A. Goedel, S. A. O. da Silva, and M. Suetake, "Scalar control of an induction motor using a neural sensorless technique," *Electric Power Systems Research*, vol. 108, pp. 322-330, 2014, doi: 10.1016/j.epsr.2013.11.020.
- [5] G. Kohlrusz and D. Fodor, "Comparison of scalar and vector control strategies of induction motors," *Hungarian Journal of Industry and Chemistry*, vol. 39, no. 2, pp. 265-270, 2011, doi: 10.1515/422.
- [6] D. L. M. Nzongo, T. Jin, G. Ekemb and L. Bitjoka, "Decoupling Network of Field-Oriented Control in Variable-Frequency Drives," *IEEE Transactions on Industrial Electronics*, vol. 64, no. 7, pp. 5746-5750, 2017, doi: 10.1109/TIE.2017.2674614.
- [7] A. Popov, V. Lapshina, F. Briz and I. Gulyaev, "Dynamic operation of FOC induction machines under current and voltage constraints," *19th European Conference on Power Electronics and Applications (EPE'17 ECCE Europe)*, 2017, pp. 1-10, doi: 10.23919/EPE17ECCEEurope.2017.8099296.
- [8] M. Kuchar, P. Brandstetter and M. Kaduch, "Sensorless induction motor drive with neural network," *IEEE 35th Annual Power Electronics Specialists Conference (IEEE Cat. No.04CH37551)*, 2004, vol. 5, pp. 3301-3305, doi: 10.1109/PESC.2004.1355058.

- [9] W. Li, Z. Xu and Y. Zhang, "Induction motor control system based on FOC algorithm," *IEEE 8th Joint International Information Technology and Artificial Intelligence Conference (ITAIC)*, 2019, pp. 1544-1548, doi: 10.1109/ITAIC.2019.8785597.
- [10] J. R. Domínguez, I. Dueñas and S. Ortega-Cisneros, "Discrete-Time Modeling and Control Based on Field Orientation for Induction Motors," *IEEE Transactions on Power Electronics*, vol. 35, no. 8, pp. 8779-8793, 2020, doi: 10.1109/TPEL.2020.2965632.
- [11] H. A. Toliyat, E. Levi and M. Raina, "A review of RFO induction motor parameter estimation techniques," *IEEE Transactions on Energy Conversion*, vol. 18, no. 2, pp. 271-283, 2003, doi: 10.1109/TEC.2003.811719.
- [12] A. Gouichiche, A. Safa, A. Chibani, and M. Tadjine, "Global fault-tolerant control approach for vector control of an induction motor," *International Transactions on Electrical Energy Systems*, vol. 30, no. 8, pp. 1-17, 2020, doi: 10.1002/2050-7038.12440.
- [13] A. A. Amin, and K. M. Hasan, "A review of fault tolerant control systems: advancements and applications," *Measurement*, vol. 143, pp. 58-68, 2019, doi: 10.1016/j.measurement.2019.04.083.
- [14] Y. Azzoug, A. Menacer, R. Pusca, R. Romary, T. Ameid and A. Ammar, "Fault Tolerant Control for Speed Sensor Failure in Induction Motor Drive based on Direct Torque Control and Adaptive Stator Flux Observer," *International Conference on Applied and Theoretical Electricity (ICATE)*, 2018, pp. 1-6, doi: 10.1109/ICATE.2018.8551478.
- [15] T. H. Yi, H. B. Huang, and H. N. Li, "Development of sensor validation methodologies for structural health monitoring: A comprehensive review," *Measurement*, vol. 109, pp. 200-214, 2017, doi: 10.1016/j.measurement.2017.05.064.
- [16] L. Baghli, P. Poure and A. Rezzoug, "Sensor fault detection for fault tolerant vector controlled induction machine," *European Conference on Power Electronics and Applications*, 2005, pp. 1-10, doi: 10.1109/EPE.2005.219346.
- [17] T. A. Najafabadi, F. R. Salmasi and P. Jabehdar-Maralani, "Detection and Isolation of Speed-, DC-Link Voltage-, and Current-Sensor Faults Based on an Adaptive Observer in Induction-Motor Drives," *IEEE Transactions on Industrial Electronics*, vol. 58, no. 5, pp. 1662-1672, 2011, doi: 10.1109/TIE.2010.2055775.
- [18] C. Chakraborty and V. Verma, "Speed and Current Sensor Fault Detection and Isolation Technique for Induction Motor Drive Using Axes Transformation," *IEEE Transactions on Industrial Electronics*, vol. 62, no. 3, pp. 1943-1954, 2015, doi: 10.1109/TIE.2014.2345337.
- [19] Y. Yu, Y. Zhao, B. Wang, X. Huang and D. Xu, "Current Sensor Fault Diagnosis and Tolerant Control for VSI-Based Induction Motor Drives," *IEEE Transactions on Power Electronics*, vol. 33, no. 5, pp. 4238-4248, 2018, doi: 10.1109/TPEL.2017.2713482.
- [20] F. Wu, J. Zhao, Y. Liu and W. Cao, "A real-time sensor fault detection, isolation and reconfiguration method for vector controlled induction motors based on Extended Kalman Filter," *International Symposium on Power Electronics, Electrical Drives, Automation and Motion (SPEEDAM)*, 2016, pp. 617-624, doi: 10.1109/SPEEDAM.2016.7525805.
- [21] C. D. Tran, P. Palacky, M. Kuchar, P. Brandstetter and B. H. Dinh, "Current and Speed Sensor Fault Diagnosis Method Applied to Induction Motor Drive," *IEEE Access*, vol. 9, pp. 38660-38672, 2021, doi: 10.1109/ACCESS.2021.3064016.
- [22] S. D. Ho, P. Brandstetter, P. Palacky, M. Kuchar, B. H. Dinh, and C. D. Tran, "Current sensorless method based on field-oriented control in induction motor drive," *Journal of Electrical Systems*, vol. 17, no. 1, pp. 62-76, 2021.
- [23] Y. Azzoug, R. Pusca, M. Sahraoui, A. Ammar, R. Romary and A. J. Marques Cardoso, "A Single Observer for Currents Estimation in Sensor's Fault-Tolerant Control of Induction Motor Drives," *International Conference on Applied Automation and Industrial Diagnostics (ICAAID)*, 2019, pp. 1-6, doi: 10.1109/ICAAID.2019.8934969.
- [24] C. D. Tran, T. X. Nguyen, P. D. Nguyen, "A field-oriented control method using the virtual currents for the induction motor drive," *International Journal of Power Electronics and Drive Systems*, vol. 12, no. 4, pp. 2095-2102, 2021, doi: 10.11591/ijpeds.v12.i4.pp2095-2102.
- [25] M. Usama, and J. Kim, "Vector control algorithm based on different current control switching techniques for Ac motor drives," *arXiv preprint arXiv:2005.04651*, 2020, doi: 10.1051/e3sconf/202015203009.

## BIOGRAPHIES OF AUTHORS



**Quang Sy Vu**    is a lecturer in Faculty of Automotive Engineering, School of Engineering and Technology, Van Lang University, Ho Chi Minh City, Vietnam. He received the B.E., M.S., and Ph.D. degrees in electrical engineering, all from Peter the Great St. Petersburg State Polytechnical University in 2012, 2014, and 2019 respectively. He can be contacted at email: sy.vq@vlu.edu.vn.



**Cuong Dinh Tran**    is a lecturer in the Electrical Engineering Department, Faculty of Electrical-Electronic Engineering at Ton Duc Thang University. He received his B.E., M.E degrees from Ho Chi Minh City University Of Technology, Vietnam, and Ph.D. degree from VSB-Technical University of Ostrava, the Czech Republic, in 2005, 2008, and 2020. His research interests include the field of modern control methods and intelligent algorithms in motor drives. He can be contacted at email: trandinhcuong@tdtu.edu.vn.



**Bach Hoang Dinh**    is the head of the Electrical Engineering Department, Faculty of Electrical-Electronic Engineering at Ton Duc Thang University. He received B.E., M.E degrees from Vietnam National University-Hochi Minh City and Ph.D. degree from Heriot-Watt University, Edinburgh, the United Kingdom, in 1995, 1998, and 2009. His research interests are intelligent and optimal control, computer vision, robotics, power electronics, SCADA, and industrial communication networks. He is a member of the IEEE Industrial Electronics Society. He can be contacted at email: [dinhhoangbach@tdtu.edu.vn](mailto:dinhhoangbach@tdtu.edu.vn).



**Chau Si Thien Dong**    is now a lecturer in the Faculty of Electrical and Electronics Engineering of Ton Duc Thang University. She received her M.Sc. and Ph.D. degrees from Ho Chi Minh City University Of Technology, Vietnam, and VSB-Technical University of Ostrava, the Czech Republic, in 2003 and 2017. Her research interests include nonlinear control, adaptive control, robust control, neural network, and the application of modern control methods in the control of electrical drives. She can be contacted at email: [dongsithienchau@tdtu.edu.vn](mailto:dongsithienchau@tdtu.edu.vn).



**Hung Tan Huynh**    is studying the Master's program in Electrical Engineering at Faculty of Electrical-Electronic Engineering, Ton Duc Thang University. He received his B.E degree from Ton Duc Thang University, Vietnam, in 2013. His research interests include the field of modern control methods and intelligent algorithms in motor drives. He can be contacted at email: [huynhtanhung@tdtu.edu.vn](mailto:huynhtanhung@tdtu.edu.vn).



**Huy Xuan Phan**    is working at Long An Power company, Long An province, Vietnam. He received his B.E., and M.E, degrees from Ho Chi Minh City University Of Technology in 2002 and 2010. His research interests include modern control methods of electrical drives, automatic control systems, intelligent control systems, and operation and control power systems. He can be contacted at email: [huypla@gmail.com](mailto:huypla@gmail.com).